IEEE Access
Multidisciplinary | Rapid Review | Open Access Journal

Received April 12, 2019, accepted April 29, 2019, date of publication May 1, 2019, date of current version May 15, 2019.

Digital Object Identifier 10.1109/ACCESS.2019.2914407

Carrier Frequency Estimation of Time-Frequency Overlapped MASK Signals for Underlay Cognitive Radio Network

MINGQIAN LIU[1], (Member, IEEE), JUNLIN ZHANG[1], YUN LIN[2], (Member, IEEE), ZHEN WU[1], BODONG SHANG[3], AND FENGKUI GONG[1], (Member, IEEE)

[1]State Key Laboratory of Integrated Service Network, Xidian University, Xi'an 710071, China
[2]College of Information and Communication Engineering, Harbin Engineering University, Harbin 150001, China
[3]Wireless@VT Group, Department of ECE, Virginia Tech, Blacksburg, VA 24061, USA

Corresponding author: Yun Lin (linyun@hrbeu.edu.cn)

This work was supported in part by the National Natural Science Foundation of China under Grant 61501348 and Grant 61801363, in part by the Shaanxi Provincial Key Research and Development Program under Grant 2019GY-043 and Grant S2019-YF-YBGY-0644, in part by the Joint Fund of Ministry of Education of China under Grant 6141A02022338, in part by the China Postdoctoral Science Foundation under Grant 2017M611912, in part by the Jiangsu Planned Projects for Postdoctoral Research Funds under Grant 1701059B, in part by the 111 Project under Grant B08038, and in part by the China Scholarship Council under Grant 201806965031.

ABSTRACT As the single-signal carrier frequency estimation method is unsuitable for the time–frequency overlapped signals in an underlay cognitive radio network (CRN), in this paper, we propose a novel carrier frequency estimation method for the time–frequency overlapped multi-level amplitude-shift keying (MASK) signals in the underlay CRN. In this method, the diagonal slice spectrum of cyclic bispectrum for the time–frequency overlapped MASK signals is first estimated, and then, the carrier frequency of component MASK signals is estimated by extracting the position information of the diagonal slice spectrum line based on the norm theory and the adaptive threshold. In addition, the Cramer–Rao bound (CRB) of the carrier frequency estimation for the time–frequency overlapped MASK signals is also derived. The simulation results show that the proposed method can estimate the carrier frequency of the time–frequency overlapped MASK signals effectively, especially in low signal-to-noise ratio (SNR) regions.

INDEX TERMS Underlay cognitive radio, carrier frequency estimation, time-frequency overlapped, cyclic bispectrum, Cramer-Rao bound.

I. INTRODUCTION

Cognitive radio (CR) behaves intelligently that the devices can obtain the spectrum information by sensing its circumambient signals and can adjust their own parameters to improve the communication performance, which is one of the effective methods to alleviate the scarcity of the available spectrum resources [1]-[2]. According to the method of spectrum access, CR is classified into overlay CR and underlay CR. In the overlay CR, secondary user (SU) can only be allowed to access to the idle licensed channel, the spectrum usage of primary user (PU) and SU cannot be overlapped in the meantime. Key technologies involved in spectrum sensing, parameter estimation [3], channel estimation [4], signal identification [5]–[8], and power allocation in the overlay CR [9]–[11]. In the underlay CR, SU can access to the licensed channel without bringing much negative impact on PU's communication, which means PU and SU can share the same spectrum simultaneously.

In the underlay CR, PU and SU share the spectrum which causes the problem that two or more time-frequency overlapped signals appear simultaneously in a general narrow band receiver. In order to avoid the interference to PU in the licensed band when a new SU accesses, it is necessary to carry out interference temperature measurement. Interference temperature is defined as a measure of the RF power available at a receiving antenna to be delivered to a receiver. This is the power generated by other transmitters and noise sources [12]. More specifically, it is the temperature equivalent of the RF power available at a receiving antenna per unit of bandwidth, measured in units of Kelvin [13]-[14]. Let f_c and B_c denote the central frequency and bandwidth (in Hertz) of the channel

The associate editor coordinating the review of this manuscript and approving it for publication was Min Jia.

c, $P_i(f_c, B_c)$ denote the interference power in Watt (at the antenna of a receiving or measuring device), and K denote the Boltzmann's constant (1.38×10^{-23} Joules per Kelvin), then the interference temperature for channel c is given by [15]

$$T_c(f_c, B_c) = -\frac{P_i(f_c, B_c)}{KB_c}. \quad (1)$$

In the interference temperature model, carrier frequency estimation is an important step in the interference temperature measurement [16]. Therefore, it is of great significance to investigate the carrier frequency estimation in underlay CR.

In recent years, parameter estimation methods for the time-frequency overlapped signals have been studied. Reference [17] proposed a method based on singular value decomposition spectrum for estimating the number of users for time-frequency overlapped signals in underlay CR. Reference [18] proposed a relay-assisted method to enable the CU to obtain the primary-link SNR by using the full-duplex relay for underlay spectrum sharing. In [19], SNR estimation was transformed into normalized power estimation of every signal component through establishing the kurtosis of time-frequency overlapped signals on the basis of second moments and forth-order moments, and this method can estimate the SNR of time-frequency overlapped signals effectively in low SNR regions. Reference [20] proposed a method to estimate the carrier frequency of overlapped signals based on second order cyclic cumulants, and the accuracy of this method is greater than 95% when signal to noise ratio (SNR) was not less than -5dB. However, this method was only applicable to BPSK, QPSK, 8QAM and 16QAM signals and failed to multi-level amplitude-shift keying (MASK) signals. MASK modulated symbols are spectrally more efficient than frequency-shift keying (FSK) signaling [21]. Furthermore, ASK is much easier to implement as compared to FSK and is less susceptible to error in wireless networks containing switching devices which create noise harmonics [22]. Therefore, in this paper, we mainly focus on the carrier frequency estimation of time-frequency overlapped MASK signals in underlay CR, which have not been fully investigated in the existing works to our best knowledge.

This paper introduces a novel carrier frequency estimation method based on diagonal slice spectrum of cyclic bispectrum for time-frequency overlapped MASK signals. The $f = 0$ slice spectrum of cyclic bispectrum is estimated first, because the carrier frequency information of time-frequency overlapped MASK signals are coexisted in this profile. Then interference suppression based on norm minimization and spectral line extraction based on adaptive threshold are carried out to dig out valuable information that can estimate the carrier frequency of component signals for the time-frequency overlapped MASK signals. Finally, the Cramer-Rao bound (CRB) of carrier frequency estimation for the time-frequency overlapped MASK signals is derived. Simulation results show that the normalized mean square error (NMSE) of the proposed estimation method is only 10^{-6} when SNR is -9 dB, which guarantees a good estimation performance under low SNR conditions.

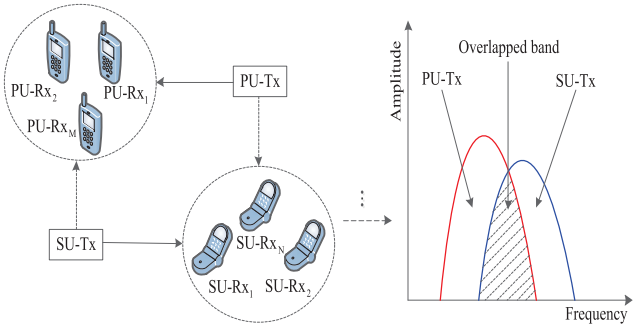

FIGURE 1. System model of underlay cognitive radio network.

The rest of this paper is organized as follows. The system and signal model is presented in Section II. The carrier frequency estimation method based on diagonal slice spectrum of cyclic bispectrum is expressed in Section III. The Cramer Rao bound (CRB) of symbol rate estimation for MASK time-frequency overlapped signals is derived in Section IV. Section V shows the numerical examples to verify the derived result and the estimation performance. Finally in Section VI we conclude the main results of this paper.

II. SYSTEM AND SIGNAL MODEL

A. SYSTEM MODEL

Fig. 1 is the system model of the underlay cognitive radio network (CRN) and shows a underlay cognitive radio system with the coexistence of primary and secondary networks where all transmissions share the same frequency band. The secondary network consists of an SU-Tx serving N SU-Rxs whereas the primary network consists of a PU-Tx communicating with M PU-Rxs [23].

B. SIGNAL MODEL

In the underlay CR, the signal model of time-frequency overlapped signals with N components is given by [21]

$$y(t) = \sum_{i=1}^{N} s_i(t) + n(t) \quad (2)$$

where $n(t)$ is zero-mean additive Gaussian noise with variance σ^2, and $s_i(t)$ $(i = 1, 2, \cdots, N)$ is the signal component of the time-frequency overlapped signals, which is expressed as

$$s_i(t) = \sum_{m=-\infty}^{+\infty} A_i a_i(m) p(t - mT_i) \cos(2\pi f_{ci} t + \phi_m) \quad (3)$$

where A_i, $a_i(m)$, f_{ci}, ϕ_m, T_i is signal amplitude, symbol sequence, carrier frequency, initial phase and symbol period, respectively. $p(t)$ is the rectangular pulse shape. We assume that the signal components and noise are independent of each other. Additionally, we assume that there is on offset in the carrier frequency of the signal.

If $s_i(t)$ is MASK signal, that is $A_i = 1$ and $\phi_i = 0$, (3) can be expressed as

$$s_i(t) = \sum_{m=-\infty}^{+\infty} a_i(m)\, p(t - mT_i) \cos 2\pi f_{ci} t \tag{4}$$

where $a_i \in \{0 \ldots M-1\}$.

III. CARRIER FREQUENCY ESTIMATION METHOD

A. DIAGONAL SLICE SPECTRUM OF CYCLIC BISPECTRUM FOR MASK SIGNAL

Cyclic bispectrum of cyclostationary signal is defined as a two-dimensional Fourier transform of third-order cyclic cumulant, which can be expressed as

$$S_{3x}^{\alpha}(f_1, f_2, \alpha) = \sum_{\tau_1=-\infty}^{+\infty} \sum_{\tau_2=-\infty}^{+\infty} C_{3x}^{\alpha}(\tau_1, \tau_2) e^{-j2\pi(f_1\tau_1 + f_2\tau_2)} \tag{5}$$

where α is the cyclic frequency of $x(t)$, τ_1 and τ_2 are different time delays, and f_1 and f_2 represent different frequency dimensions.

Cyclic bispectrum is a multi-dimensional distribution of f_1, f_2 and α. When $f_1 = f_2$, we can get its diagonal slice spectrum. It is also called $1\frac{1}{2}$ spectrum whose expression is

$$S_{3x}^{\alpha}(f) = \sum_{\tau=-\infty}^{+\infty} C_{3x}^{\alpha}(\tau) e^{-j2\pi f \tau} \tag{6}$$

So (3) can be rewritten as

$$s_i(t) = z_i(t) w_i(t) \tag{7}$$

where $z_i(t) = \sum_{m=-\infty}^{+\infty} a_i(m)\, p(t - mT_i)$ and $w_i(t) = \cos 2\pi f_{ci} t$.

In order to facilitate the theoretical analysis, we analyze the cyclic bispectrum diagonal spectrum of single MASK, firstly. According to [24], the relationship of cycle bispectrum diagonal spectrum of two multiplied signals can be expressed as

$$S_s^{\alpha}(f) = \sum_{\beta} \int_{-\infty}^{+\infty} S_z^{\alpha-\beta}(f - v) S_w^{\beta}(v) dv \tag{8}$$

where α and β are cyclic frequencies of $s(t)$ and $f(t)$ respectively. By substituting $w(t) = \cos 2\pi f_c t$ into (6), the expression of the bispectrum diagonal spectrum can be easily expressed as

$$S_w^{\beta}(f) = \begin{cases} \frac{\pi}{2}\delta(f) + \frac{\pi}{4}\delta(f - 2f_c), & \beta = f_c \\ \frac{\pi}{4}\delta(f - 2f_c), & \beta = 3f_c \\ 0, & others \end{cases} \tag{9}$$

By substituting $z(t) = \sum_{m=-\infty}^{+\infty} a(m)\, p(t - mT)$ and (9) into (8), we can obtain the cyclic bispectrumdiagonal spectrum of single MASK as

$$\begin{aligned} S_s^{\alpha}(f) &= \sum_{\beta} \int_{-\infty}^{+\infty} S_z^{\alpha-\beta}(f - v) S_w^{\beta}(v) dv \\ &= \sum_{\beta=f_c, 3f_c} \int_{-\infty}^{+\infty} S_z^{\alpha-\beta}(f - v) S_w^{\beta}(v) dv \\ &= \int_{-\infty}^{+\infty} S_z^{\alpha-f_c}(f - v) S_w^{f_c}(v) + S_z^{\alpha-3f_c}(f - v) S_w^{3f_c}(v) dv \\ &= \int_{-\infty}^{+\infty} S_z^{\alpha-f_c}(f - v) \left[\frac{\pi}{2}\delta(v) + \frac{\pi}{4}\delta(v - 2f_c)\right] dv \\ &\quad + \int_{-\infty}^{+\infty} S_z^{\alpha-3f_c}(f - v) \frac{\pi}{4}\delta(v - 2f_c) dv \\ &= \frac{\pi}{2} S_z^{\alpha-f_c}(f) + \frac{\pi}{4}\left(S_z^{\alpha-f_c}(f - 2f_c) + S_z^{\alpha-3f_c}(f - 2f_c)\right) \end{aligned} \tag{10}$$

Then, how to obtain the cyclic bispectral diagonal spectrum of the baseband signal is a problem that deserves attention.

According to [25], we know that cyclic polyspectra of $z(t)$ can be expressed as

$$S_z^{\gamma}\left(\vec{f}\right)_n = \frac{c_{a,n}}{T} P\left(\gamma - 1^{+}\vec{f}\right) \prod_{j=1}^{n=1} P\left(f_j\right) \tag{11}$$

where $c_{a,n}$ is the n-th order moment of $a(t)$ and it is constant. $P(f)$ is the Fourier transform of the rectangular pulse $p(t)$. $\vec{f} = (f_1, f_2 .. f_{n-1})$ while 1^{+} means a (n-1)-dimensional column vector, $\gamma = k/T$, $k = 0, 1, 2, \cdots$ is the cyclic frequency of $z(t)$. By substituting $n = 3$ into (11), we can obtain the expression of cyclic bispectrum of $z(t)$

$$S_z^{\gamma}(f_1, f_2)_3 = \frac{c_{a,3}}{T} P(\gamma - f_1 - f_2) P(f_1) P(f_2) \tag{12}$$

When $f_1 = f_2 = f$, (12) can be expressed as

$$S_z^{\gamma}(f) = \frac{c_{a,3}}{T} P(\gamma - 2f) P(f)^2 \tag{13}$$

We can obtain the expression of $S_z^{\alpha-f_c}(f)$, $S_z^{\alpha-f_c}(f - 2f_c)$ and $S_z^{\alpha-3f_c}(f - 2f_c)$ as following,

$$S_z^{\alpha-f_c}(f) = \frac{c_{a,3}}{T} P(\alpha - 2f - f_c) P(f)^2, \alpha - f_c = k/T \tag{14}$$

$$\begin{aligned} S_z^{\alpha-f_c}(f - 2f_c) &= \frac{c_{a,3}}{T} P(\alpha - f_c - 2f + 4f_c) P(f - 2f_c)^2 \\ &= \frac{c_{a,3}}{T} P(\alpha - 2f + 3f_c) P(f - 2f_c)^2, \alpha - f_c = \frac{k}{T} \end{aligned} \tag{15}$$

$$\begin{aligned} S_z^{\alpha-3f_c}(f - 2f_c) &= \frac{c_{a,3}}{T} P(\alpha - 3f_c - 2f + 4f_c) P(f - 2f_c)^2 \\ &= \frac{c_{a,3}}{T} P(\alpha - 2f + f_c) P(f - 2f_c)^2, \alpha - 3f_c = \frac{k}{T} \end{aligned} \tag{16}$$

By substituting (14), (15) and (16) into (10), we can obtain

$$\begin{aligned} S_s^{\alpha}(f) = \Big[& 2\varsigma P(\alpha - 2f - f_c)P^2(f) \\ & + \varsigma P(\alpha+3f_c)P^2(f-2f_c)]\delta(\alpha-f_c-k/T) \\ & +\varsigma P(\alpha-2f+f_c)P^2(f-2f_c)\delta(\alpha-3f_c-k/T) \end{aligned} \quad (17)$$

where $\varsigma = \frac{\pi c_{a,3}}{2T}$ is a constant value for modulation.

Let $f = 0$, the cyclic frequency section of cyclic bispectrum diagonal is given by

$$\begin{aligned} S_s^{\alpha}(0) = & [2\varsigma P(\alpha - f_c) \\ & +\varsigma P(\alpha + 3f_c)P^2(2f_c)]\delta(\alpha - f_c - k/T) \\ & +\varsigma P(\alpha + f_c)P^2(2f_c)\delta(\alpha - 3f_c - k/T) \\ = & [2\varsigma P(k/T) \\ & +\varsigma P(4f_c + k/T)P^2(2f_c)]\delta(\alpha - f_c - k/T) \\ & +\varsigma P(4f_c + k/T)P^2(2f_c)\delta(\alpha - 3f_c - k/T) \end{aligned} \quad (18)$$

where $P(f) = \frac{\sin \pi f T}{\pi f}$ and $P(k/T) = T\frac{\sin \pi k}{\pi k}, k = 0, 1, 2, \cdots$. $P(k/T)$ can reach maximum value when $k = 0$, (18) can be expressed as

$$\begin{aligned} S_s^{\alpha}(0) = & \varsigma[2P(0) + P(4f_c)P^2(2f_c)]\delta(\alpha - f_c) \\ & +\varsigma P(4f_c)P^2(2f_c)\delta(\alpha - 3f_c) \end{aligned} \quad (19)$$

From (19), we can see that there is two impulses on the cyclic frequency axis of the cyclic bispectrum slice spectrum $f = 0$ section for MASK signal, and $S_s^{\alpha}(0)$ reaches the maximum value when $\alpha = f_c$. Therefore, the carrier frequency of a single MASK signal can be estimated by searching the position of the max impulse.

B. DIAGONAL SLICE SPECTRUM OF CYCLIC BISPECTRUM FOR TIME-FREQUENCY OVERLAPPED MASK SIGNALS

Accroding to the signal model in (2), we can assume that there are two signal components altogether. Each signal is zero-mean and is independent of each other. The cyclic double correlation function can be written as

$$\begin{aligned} R_y^{\alpha}(\tau) = & < \{s_1(t) + s_2(t)\} \\ & \cdot\{s_1(t+\tau) + s_2(t+\tau)\}^2 >_t e^{-j2\pi\alpha t} \\ = & < \{s_1(t)s_1^2(t+\tau) + 2s_1(t)s_1(t+\tau)s_2(t+\tau) \\ & + 2s_2(t)s_1(t+\tau)s_2(t+\tau) + s_1(t)s_2^2(t+\tau) \\ & + s_2(t)s_2^2(t+\tau) + s_2(t)s_1(t+\tau)^2\} >_t e^{-j2\pi\alpha t} \end{aligned} \quad (20)$$

where $< \cdot >_t = \lim_{T_0 \to 0} \frac{1}{T}\int_{-T/2}^{T/2} \cdot dt$. Since $s_1(t)$ and $s_2(t)$ are independent of each other, (20) can be given by

$$\begin{aligned} & R_y^{\alpha}(\tau) \\ & = < \left[s_1(t)\, s_1^2(t+\tau) + s_2(t)\, s_2^2(t+\tau) \right] >_t e^{-j2\pi\alpha t} \\ & = R_{s1}^{\alpha}(\tau) + R_{s2}^{\alpha}(\tau) \end{aligned} \quad (21)$$

The cyclic bispectrum diagonal spectrum of time-frequency overlapped double-signal is obtained by performing Fourier transform on (21), as follows

$$S_y^{\alpha}(f) = S_{s1}^{\alpha}(f) + S_{s2}^{\alpha}(f) \quad (22)$$

(22) shows that the time-frequency overlapped double-signal cyclic bispectrum diagonal spectrum satisfies linear superposition. Thus, the time-frequency MASK signal overlapped cyclic bispectrum diagonal spectrum is given by

$$\begin{aligned} S_y^{\alpha}(f) = & \sum_{i=1}^{N} S_{s_i}^{\alpha}(f) \\ = & \sum_{i=1}^{N} \{[2\varsigma_i P(\alpha - 2f - f_{ci})P^2(f) \\ & +\varsigma_i P(\alpha+3f_{ci})P^2(f-2f_{ci})]\delta(\alpha-f_{ci}-k/T_i) \\ & +\varsigma_i P(\alpha-2f+f_{ci})P^2(f-2f_{ci})\delta(\alpha-3f_{ci}-k/T_i)\} \end{aligned} \quad (23)$$

where N represent the number of signal components. Substituting $f = 0$ into (23), we can obtain

$$\begin{aligned} S_y^{\alpha}(0) = & \sum_{i=1}^{N} [2\varsigma_i P(k/T_i) \\ & +\varsigma_i P(4f_{ci}+k/T_i)P^2(2f_{ci})]\delta(\alpha-f_{ci}-k/T_i) \\ & +\varsigma_i P(4f_{ci}+k/T_i)P^2(2f_{ci})\delta(\alpha-3f_{ci}-k/T_i) \end{aligned} \quad (24)$$

$P(K/T)$ can reach maximum value when $k = 0$ and (24) can be expressed as

$$\begin{aligned} S_y^{\alpha}(0) = & \sum_{i=1}^{N} [2\varsigma_i P(0)+\varsigma_i P(4f_{ci})P^2(2f_{ci})]\delta(\alpha-f_{ci}) \\ & +\varsigma_i P(4f_{ci})P^2(2f_{ci})\delta(\alpha - 3f_{ci}) \end{aligned} \quad (25)$$

C. SPECTRAL LINE EXTRACTION OF DIAGONAL SLICE SPECTRUM

Due to the interference and noise, there are many clutter lines in the cross section of $f = 0$ slice of the cyclic bispectrum diagonal spectrum, so that it is difficult to extract carrier frequency information. Therefore, the spectral lines need to be pre-processed.

L-norm can be used to suppresses noise and spurious peaks. The 0-norm does not reduce the peak value when small discrete lines are filtered out, and the smaller spectral lines becomes cleaner. Therefore, the problem of spectral line pretreatment is transformed into L_0-norm minimization problem. We assume that c is the vector of spectral lines to be processed and d is the vector of processed spectrum that is the desired optimal solution. Φ is the measurement matrix. The sparse vector d can be obtained by solving the following problem

$$\min \|\mathbf{d}\|_0 \quad s.t. \|\Phi\mathbf{c} - \Phi\mathbf{d}\|_2 \leq \varepsilon \quad (26)$$

where $\|\cdot\|_2$ and $\|\cdot\|_0$ are respectively 2-Norm and 0-Norm of a vector.

It's worth noting that the above problem is NP-hard and it can be written in s simple form sparse denoising [13], [26].

$$\min \left(\|\Phi\mathbf{c} - \Phi\mathbf{d}\|_2^2 + \|\mathbf{d}\|_0 \right) \quad (27)$$

The optimal solution in (27) can be obtained by the fastest gradient descent methodology, so as to achieve the pretreatment of spectral lines.

After the pretreatment, setting the local threshold adaptively can weaken the omission of strong spectral lines and avoid the appearance of pseudo-spectral lines. In this paper, the thresholds within each window are adaptively set to extract discrete spectral lines. The specific method is shown as follows. First, we choose a window of certain length to calculate the standard deviation of the spectral amplitude in the window. Second, the local threshold of the window is $\mu \times \sigma$ (μ is a constant). Third, the rid of lines are obtained which are less than $\mu \times \sigma$, while leaving lines greater than the threshold. The standard deviation of the line amplitude is expressed as

$$\sigma = \left[\frac{\sum_{i=1}^{R} \left(\left| |S(f_i)| - \frac{1}{R} \sum_{i=1}^{R} |S(f_i)| \right| \right)^2}{(R-1)} \right]^{1/2} \tag{28}$$

where R is the number of spectral lines in a window, $|S(f)|$ is the amplitude of spectral lines. After the above processing, sparse and clear spectral lines can be obtained. Then solve the ratio of intensity to mean of the spectral lines in each window, which can be expressed as

$$|N(f_i)| = \frac{|S(f_i)|}{\frac{1}{R} \sum_{i=1}^{R} |S(f_i)|} \tag{29}$$

Then search the maximum value $|N(f_0)|$ in each window, where f_0 is the frequency relating to the maximum value. Sort these maximum values of all windows. Next, we select the top N large values, corresponding to the number of time-frequency overlapped frequency signal components. And frequencies that relates to the N large values are chosen as the carrier frequencies of the time-frequency overlapped MASK signals. In summary, the spectral line extraction method is illustrated as follows. First, the discrete lines are pre-processed based on L_0-norm minimization in order to reduce noise and enhance spectral lines, and then set the local threshold based on standard deviation of the spectral lines in each window and get rid of lines below the threshold. Finally, obtain the time-frequency overlapped MASK signals carrier frequency by searching for the local maximum point.

The procedure of carrier frequency estimation for the time-frequency overlapped MASK signals in underlay CR is summarized in Algorithm 1.

Algorithm 1 The procedure of carrier frequency estimation for time-frequency overlapped MASK signals in underlay CR.

1: Calculate the cyclic bispectrum diagonal slices spectrum of the received overlapped signals according to (6).
2: Noise reduction and spectral lines enhancement by solving (27).
3: Add window to the spectral segment and set the local threshold by using (28). Then keep the discrete lines above the threshold value.
4: Use (29) to calculate the ratio of intensity to mean and search the local maximum values in each window, then sort these values.
5: Select top N maximum values according to the number of time-frequency overlapped signal components. Frequencies related to these values are acted as carrier frequencies of the overlapped MASK signals.

IV. CRB OF CARRIER FREQUENCY ESTIMATION FOR TIME-FREQUENCY OVERLAPPED MASK SIGNALS

Based on (2), time-frequency overlapped signals with N components can be rewritten as

$$y(t) = \sum_{i=1}^{N} s_i(t) + n(t) = \sum_{i=1}^{N} z_i(t) \exp(j2\pi f_{ci} t) + n(t) \tag{30}$$

And the k-th symbol of MASK can be expressed as

$$y_k = \sum_{i=1}^{N} z_{i,k} \exp(j2\pi f_{ci} k T_i) + n_k \tag{31}$$

where $z_{i,k}$ is the i-th baseband signal of k-th signal component

The log likehood function of y_k with M samples is

$$\ln p(y|f_{c1}, f_{c2}..f_{cN}) = -\frac{1}{\sigma^2} \sum_{k=1}^{M} \left| y_k - \sum_{i=1}^{N} z_{i,k} \exp(j2\pi f_{ci} k T_i) \right| \tag{32}$$

After a derivative mathematical operation of f_{ci}, we obtain

$$\frac{\partial \ln p(y|f_{c1}, f_{c2}..., f_{cN})}{\partial f_{ci}} = -\frac{2\pi T_i}{\sigma^2} \sum_{k=1}^{M} \left| \left\{ y_k - \sum_{i=1}^{N} z_{i,k} \exp(j2\pi f_{ci} k T_i) \right\} z_{i,k} k \right| \tag{33}$$

Substituting $n_k = y_k - \sum_{i=1}^{N} z_{i,k} \exp(j2\pi f_{ci} k T_i)$ into (33), we can obtain

$$\frac{\partial \ln p(y|f_{c1}, f_{c2}..., f_{cN})}{\partial f_{ci}} = -\frac{2\pi T_i}{\sigma^2} \sum_{k=1}^{M} |n_k z_{i,k} k| \tag{34}$$

The element of Fisher matrix $\mathbf{F}$ can be calculated as

$$E\left[\frac{\partial \ln p(y|f_{c1}, f_{c2}..., f_{cN})}{\partial f_{ci}} \cdot \frac{\partial \ln p(y|f_{c1}, f_{c2}..., f_{cN})}{\partial f_{cj}} \right] = E\left[\frac{4\pi^2 T_i T_j}{\sigma^4} \sum_{k=1}^{M} |n_k z_{i,k} k| \sum_{v=1}^{M} |n_v z_{j,v} v| \right] \tag{35}$$

$$E\left[\frac{\partial \ln p(y|f_{c1}, f_{c2}..., f_{cN})}{\partial f_{ci}} \cdot \frac{\partial \ln p(y|f_{c1}, f_{c2}..., f_{cN})}{\partial f_{cj}} \right] = \frac{4\pi^2 T_i T_j}{\sigma^4} E\left[\sum_{k=1}^{M} \sum_{v=1}^{M} |n_k z_{i,k} k| \, |n_v z_{j,v} v| \right]$$

$$= \frac{4\pi^2 T_i T_j}{\sigma^4} \sum_{k=1}^{M} \sum_{v=1}^{M} E\left[|n_k n_v| \left|z_{i,k} z_{j,v}\right| kv\right]$$
$$= \frac{4\pi^2 T_i T_j}{\sigma^4} \sum_{k=1}^{M} \sum_{v=1}^{M} \sigma^2 \delta(k-v) kv E\left[z_{i,k} z_{j,v}\right] \quad (36)$$

Because each component signal is independent and $E[z_{i,k}z_{j,v}] = 0$, according to (35) and (36), we can obtain the Fisher matrix

$$\mathbf{F} = \begin{bmatrix} E[\frac{\partial \ln p(y|f_{c1},f_{c2}\ldots,f_{cN})}{\partial f_{c1}}^2] & & \\ & \ddots & \\ & & E[\frac{\partial \ln p(y|f_{c1},f_{c2}\ldots,f_{cN})}{\partial f_{cN}}^2] \end{bmatrix} \quad (37)$$

where

$$\mathbf{F}_{ii} = \frac{4\pi^2 T_i^2}{\sigma^2} \sum_{k=1}^{M} k^2 E[z_{i,k}^2]$$
$$= \frac{2M(M+1)(2M+1)\pi^2 T_i^2}{3\sigma^2} E[z_i^2] \quad (38)$$

If the power ratio of each component is $\gamma_1 : \gamma_2 \ldots : \gamma_N$ and $SNR = \frac{E[y^2]}{\sigma^2}$, we have

$$\frac{E[z_i^2]}{\sigma^2} = \frac{\gamma_i}{\gamma_1+\gamma_2+\ldots+\gamma_N} \frac{E[y^2]}{\sigma^2}$$
$$= \frac{\gamma_i}{\gamma_1+\gamma_2+\ldots+\gamma_N} SNR \quad (39)$$

Assume that $\gamma = \gamma_i / (\gamma_1+\gamma_2+\ldots+\gamma_N)$. By substituting (39) into (38), the CRB of the i-th component can be obtained as follows

$$CRB\hat{f}_{ci} = \frac{1}{\mathbf{F}_{ii}} = \frac{3\gamma}{2\pi^2 T_i^2 M(M+1)(2M+1)} \frac{1}{SNR} \quad (40)$$

and we can define the normalized Cramer-Rao bound (NCRB) of f_{ci} with the i-th component as

$$NCRB\hat{f}_{ci} = \frac{CRB\hat{f}_{ci}}{f_{ci}^2} \quad (41)$$

V. NUMERIC SIMULATION AND DISCUSSION

In this section, we show the simulation results and the analysis which are to evaluate the performance of the frequency estimation method. We take 8000 samples as a trial source and do a variety of simulations in MATLAB to assess the performance of the proposed frequency estimation method for time-frequency overlapped MASK signals in underlay CR. We assume that the signal components and noise are independent of each other. The signal model is time-frequency overlapped with $\alpha = 0.35$, and the AWGN channel is considered. The normalized mean square error (NMSE) is used to evaluate the performance of the proposed method by 2000 Monte Carlo experiments, and NMSE is defined as

$$NMSE = \left|\hat{f}_c - f_c\right|^2 \Big/ f_c^2 \quad (42)$$

where f_c is the real frequency and $\hat{f}_c$ is the estimated value.

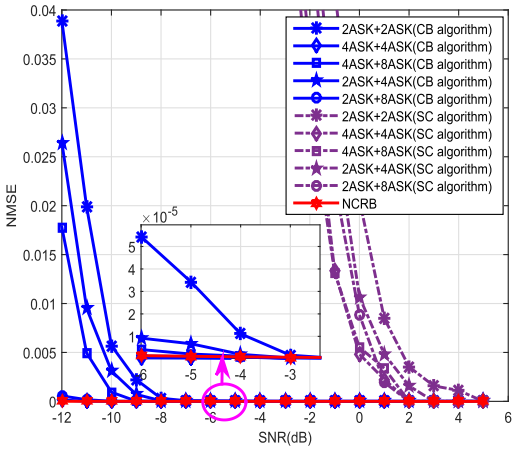

FIGURE 2. Carrier frequency estimation performance varies with SNR of two signals.

In order to verify the influence of SNR on carrier frequency estimation performance of the overlapped signals, we conduct the simulation with two and three signals respectively and observe how the performance varies with SNR. Modulation modes of the signal component are 2ASK, 4ASK and 8ASK. Different modulation combinations of two or three signals are chosen to conduct the experiments. We set $f_b = 400$ Baud, $f_s = 4000$ Hz, the spectral overlapped ratio is 50% and each component has the same power, $\gamma_1 : \gamma_2 = 1 : 1$ or $\gamma_1 : \gamma_2 : \gamma_3 = 1 : 1 : 1$. For two signals, $f_{c1} = 300$ Hz and $f_{c2} = 500$ Hz. For three signals $f_{c1} = 300$ Hz, $f_{c2} = 500$ Hz and $f_{c3} = 600$ Hz.

For two signals, the spectral overlapped ratio is defined as

$$\xi = \frac{B_{overlapped}}{\min(B_1, B_2)} \quad (43)$$

where $B_{overlapped}$ is the overlapped spectral width of two signals, B_1 and B_2 are spectral width of signal components, respectively.

In Fig.2, the proposed method based on the cyclic bispectrum (CB) algorithm is compared with the method based on the cyclostationarity (SC) algorithm. we set the same simulation parameters for the above two methods. As can be seen in Figs.2, CB algorithm has a higher success probability than the SC algorithm in low SNR regions. The performance of the CB algorithm is very close to the NCRB after -8dB. However, the performance of the SC algorithm is very close to the NCRB after 2dB. In other words, the CB algorithm has better performance than the SC algorithm in the lower SNR regions. In addition, we analyze the computational complexity of the above two methods. The computational complexity of the CB algorithm and SC algorithm are $O\left(N^3 log_2 N\right)$ and $O\left(N^2 log_2 N\right)$, respectively. Although the proposed method has higher computational complexity, it achieves better performance in terms of the carrier frequency estimation.

In Fig.2 and Fig.3, we can see that the average NMSE of the carrier frequency estimation decreases gradually with the increase of SNR. The proposed method can effectively

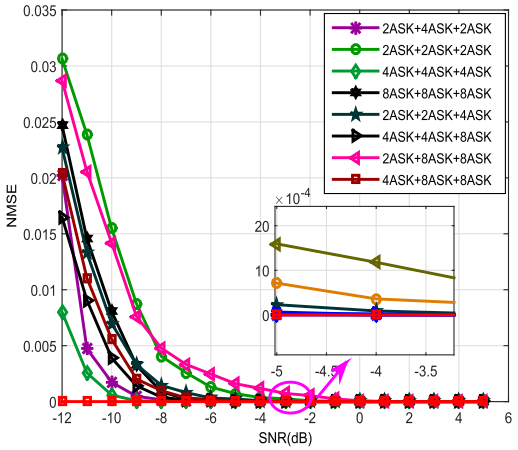

FIGURE 3. Carrier Frequency Estimation Performance varies with SNR of three signals.

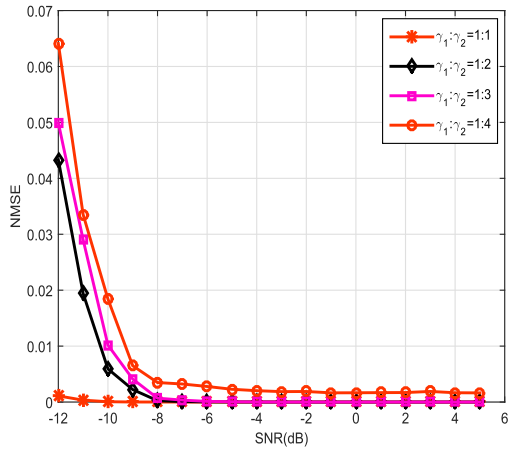

FIGURE 4. Carrier frequency estimation performance varies with power ratio of two signals.

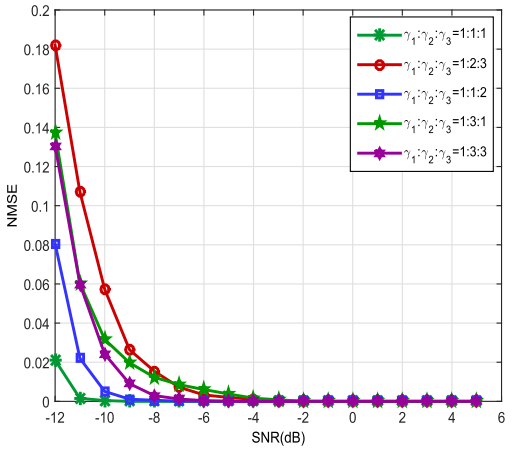

FIGURE 5. Carrier frequency estimation performance varies with power ratio of three signals.

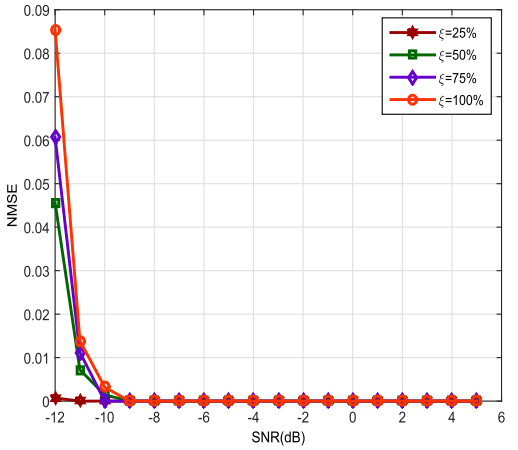

FIGURE 6. Carrier frequency estimation performance varies with overlapped ratio.

estimate the carrier frequency of the time-frequency overlapped signals. Our proposed carrier frequency estimation method is found to clearly offer a good overall performance, essentially achieving the NCRB.

In order to verify the influence of the power ratio of each component on carrier frequency estimation performance, we conduct the simulation with two and three signals respectively and we observe the performance varying with power ratio. The signal component modulation modes are 2ASK and 4ASK. We set $f_b = 400$ Baud, $f_s = 4000$ Hz, the spectral overlapped ratio is 50%. For two signals, $f_{c1} = 300$ Hz and $f_{c2} = 500$ Hz. For three signals $f_{c1} = 300$ Hz, $f_{c2} = 500$ Hz and $f_{c3} = 600$ Hz. Fig.4 and Fig.5 show the carrier estimation' s average NMSE of two and three overlapped signals, respectively.

From Fig.4 and Fig.5, we can see that the performance of carrier estimation is degraded with signal ratio difference increasing, regardless of two or three signals. However, the worst performance can still effectively estimate the carrier frequency. As a result, the proposed method has robustness to the power ratio.

The final simulation is to verify the signal overlapped rate effect on the carrier frequency estimation. Signal parameters are set as follows. The modulated types are 2ASK and 4ASK, $f_{c1} = 300$ Hz and $f_{c2} = 500$ Hz, the power ratio is $\gamma_1{:}\gamma_2 = 1:1$, f_b varies with the overlapped ratio. The results are shown in Fig.6. We can draw the conclusion that the estimation performance is degraded with the increase of spectrum overlapped ratio. The best performance is obtained when the overlapped rate is 25%. The overlapped ratio directly affects the carrier frequency estimation of time-frequency overlapped MASK signals. When the overlapped ratio is 100% and SNR is -9dB, the NMSE is 10^{-6}, we can see that the proposed method has the robustness to spectrum overlapped ratio.

VI. CONCLUSION

Underlay CR can effectively improve the spectrum utilization, but carrier frequency estimation is an important part in the interference temperature measurement of underlay CR. In this paper, we have presented a novel carrier frequency estimation method for the time-frequency overlapped MASK signals in underlay CR. This method can estimate the carrier frequency effectively by utilizing diagonal slice spectrum

of cyclic bispectrum. The optimization algorithm based on norm minimization and local adaptive threshold are used to improve the estimation performance. Moreover, the CRB of the carrier frequency estimation for time-frequency overlapped MASK signals is also analyzed. From numerical results, it is verified that this proposed carrier frequency estimation method has promising and robust performance.

REFERENCES

[1] M. Jia, X. Gu, Q. Guo, W. Xiang, and N. Zhang, "Broadband hybrid satellite-terrestrial communication systems based on cognitive radio toward 5G," *IEEE Wirless Commun.*, vol. 23, no. 6, pp. 96–106, Dec. 2016.

[2] M. Jia, X. Liu, X. Gu, and Q. Guo, "Joint cooperative spectrum sensing and channel selection optimization for satellite communication systems based on cognitive radio," *Int. J. Sat. Commun. Netw.*, vol. 35, no. 2, pp. 139–150, Mar./Apr. 2017.

[3] M. Jia, Z. Yin, Q. Guo, G. Liu, and X. Gu, "Waveform design of zero head DFT spread spectral efficient frequency division multiplexing," *IEEE Access*, vol. 5, pp. 16944–16952, 2016.

[4] X. Li, N. Zhao, Y. Sun, and F. R. Yu, "Interference alignment based on antenna selection with imperfect channel state information in cognitive radio networks," *IEEE Trans. Veh. Technol.*, vol. 65, no. 7, pp. 5497–5511, Jul. 2016.

[5] Z. Zhang, X. Guo, and Y. Lin, "Trust management method of D2D communication based on RF fingerprint identification," *IEEE Access*, vol. 6, pp. 66082–66087, 2018.

[6] Y. Tu, Y. Lin, J. Wang, and J. U. Kim, "Semi-supervised learning with generative adversarial networks on digital signal modulation classification," *Comput. Mater. Continua*, vol. 55, no. 2, pp. 243–254, May 2018.

[7] H. Wang, L. Guo, Z. Dou, and Y. Lin, "A new method of cognitive signal recognition based on hybrid information entropy and D-S evidence theory," *Mobile Netw. Appl.*, vol. 23, no. 4, pp. 677–685, Aug. 2018.

[8] Y. Lin, X. Zhu, Z. Zheng, Z. Dou, and R. Zhou, "The individual identification method of wireless device based on dimensionality reduction and machine learning," *J. Supercomput.*, 2017. doi: 10.1007/s11227-017-2216-2.

[9] Y. Cao *et al.*, "Optimization or alignment: Secure primary transmission assisted by secondary networks," *IEEE J. Sel. Areas Commun.*, vol. 36, no. 4, pp. 905–917, Apr. 2018.

[10] H. Song and X. Fang, "A spectrum etiquette protocol and interference coordination for LTE in unlicensed bands (LTE-U)," in *Proc. IEEE Int. Conf. Commun. Workshop (ICCW)*, London, U.K., Jun. 2015, pp. 2338–2343.

[11] N. Zhao, F. Yu, H. Sun, and M. Li, "Adaptive power allocation schemes for spectrum sharing in interference-alignment-based cognitive radio networks," *IEEE Trans. Veh. Technol.*, vol. 65, no. 5, pp. 3700–3714, May 2016.

[12] H. Song, X. Fang, and C.-X. Wang, "Cost-reliability tradeoff in licensed and unlicensed spectra interoperable networks with guaranteed user data rate requirements," *IEEE J. Sel. Areas Commun.*, vol. 35, no. 1, pp. 200–214, Jan. 2017.

[13] "In the matter of establishment of an interference metric to quantify and manage interference and to expand available unlicensed operation in certain fixed, mobile and satellite frequency bands," Federal Commun. Commission, Tech. Rep. FCC 03-289, Nov. 2003.

[14] T. C. Clancy, "Formalizing the interference temperature model," *Wireless Commun. Mobile Comput.*, vol. 7, no. 9, pp. 1077–1086, Nov. 2007.

[15] M. Sharma, A. Sahoo, and K. D. Nayak, "Channel modeling based on interference temperature in underlay cognitive wireless networks," in *Proc. IEEE Int. Symp. Wireless Commun. Syst.*, Oct. 2008, pp. 224–228.

[16] B. Jalaeian, R. Zhu, H. Samani, and M. Motani, "An optimal cross-layer framework for cognitive radio network under interference temperature model," *IEEE Syst. J.*, vol. 10, no. 1, pp. 293–301, Mar. 2016.

[17] Y. Shi, M. Liu, and F. Zhou, "User numbers estimation for underlay cognitive radio," in *Proc. 6th Int. Conf. Wireless, Mobile Multi-Media*, Nov. 2015, pp. 120–123.

[18] G. Zhao, B. Huang, L. Li, and Z. Chen, "Estimate the primary-link SNR using full-duplex relay for underlay spectrum sharing," *IEEE Signal Process. Lett.*, vol. 23, no. 4, pp. 429–433, Apr. 2016.

[19] J. Wang, B. Li, M. Liu, and J. Li, "SNR estimation of time-frequency overlapped signals for underlay cognitive radio," *IEEE Commun. Lett.*, vol. 19, no. 11, pp. 1925–1928, Nov. 2015.

[20] M. Gong and R. Guo, "A novel spectrum utilization method for cognitive radio applications," in *Proc. Int. Conf. Multimedia Commun.*, Aug. 2010, pp. 71–74.

[21] S. P. Dash, R. K. Mallik, and S. K. Mohammed, "Performance analysis of non-coherent PLC with multi-level ASK in impulsive noise environment," *IET Commun.*, vol. 12, no. 7, pp. 816–823, Apr. 2018.

[22] A. Dubey, D. Sharma, R. K. Mallik, and S. Mishra, "Modeling and performance analysis of a PLC system in presence of impulsive noise," in *Proc. IEEE Power Energy Gen. Meeting*, Jul. 2015, pp. 1–5.

[23] M. Liu, J. Zhang, and B. Li, "Symbol rates estimation of time-frequency overlapped MPSK signals for underlay cognitive radio network," *IEEE Access*, no. 6, pp. 16216–16223, 2018.

[24] W. Gardner, "Spectral correlation of modulated signals: Part I—Analog modulation," *IEEE Trans. Commun.*, vol. 35, no. 6, pp. 584–594, Jun. 1987.

[25] W. Gardner, W. Brown, and C.-K. Chen, "Spectral correlation of modulated signals: Part II—Digital modulation," *IEEE Trans. Commun.*, vol. 35, no. 6, pp. 595–601, Jun. 1987.

[26] Y. Tsaig and D. L. Donoho, "Extensions of compressed sensing," *Signal Process.*, vol. 86, no. 3, pp. 549–571, Mar. 2006.

MINGQIAN LIU (M'13) received the B.S. degree in electrical engineering from Information Engineering University, in 2006, the M.S. degree from the Xi'an University of Technology, in 2009, and the Ph.D. degree in communication and information system from Xidian University, Xi'an, China, in 2013, where he is currently with the State Key Laboratory of Integrated Services Networks and did postdoctoral research, from 2014 to 2016. His research interests include communication signal processing, statistical signal processing, and cognitive radio.

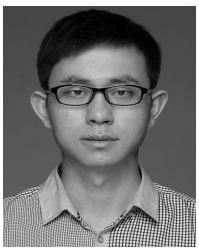

JUNLIN ZHANG received the M.S. degree in information and communication engineering from Information Engineering University, Zhengzhou, China, in 2017. He is currently pursuing the Ph.D. degree in communication and information system with Xidian University. His current research interests include communication signal processing and cognitive radio.

YUN LIN received the B.S. degree from Dalian Maritime University, in 2003, the M.S. degree from the Harbin Institute of Technology, in 2005, and the Ph.D. degree from Harbin Engineering University, in 2010. He was a Visiting Scholar with Wright State University, Dayton, OH, USA, from 2014 to 2015. He is currently an Associate Professor with Harbin Engineering University. His research interests include communication technology, signal processing, information fusion, cognitive radio, and software-defined radio.

ZHEN WU received the B.S. and M.S. degrees from Xidian University, in 2013 and 2017, respectively. Her current research interests include communication signal processing and cognitive radio.

BODONG SHANG received the B.S. degree in communication engineering from Northwest University, Xi'an, China, in 2015, and the M.S. degree in communication and information system from Xidian University, Xi'an, in 2018. He is currently pursuing the Ph.D. degree in electrical and computer engineering with Virginia Tech, Blacksburg, USA. His recent research interests include several aspects of wireless communication, such as MIMO systems, device-to-device communication, edge computing and caching, and the IoT.

FENGKUI GONG received the M.S. and Ph.D. degrees from Xidian University, Xi'an, China, in 2004 and 2007, respectively. From 2011 to 2012, he was a Visiting Scholar with the Department of Electrical and Computer Engineering, McMaster University, Hamilton, ON, Canada. He is currently a Professor with the State Key Laboratory of Integrated Services Networks, Department of Communication Engineering, Xidian University. His research interests include cooperative communication, distributed space–time coding, digital video broadcasting systems, satellite communication, and 4G/5G techniques.